NASA Technical Memorandum 83422

Wear Particle Analysis Using the Ferrograph

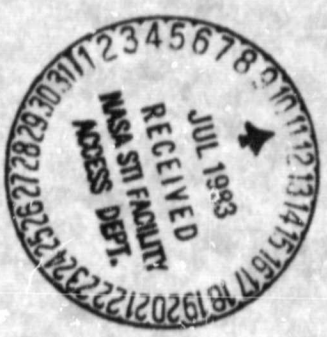

William R. Jones, Jr.
Lewis Research Center
Cleveland, Ohio

Prepared for the
Joint Meeting of the Fluid Power Society and the
American Society of Lubrication Engineers
Detroit, Michigan, April 26, 1983

NASA

WEAR PARTICLE ANALYSIS USING THE FERROGRAPH

William R. Jones, Jr.

National Aeronautics and Space Administration
Lewis Research Center
Cleveland, Ohio

ABSTRACT

The use of the Ferrograph in analyzing wear particles from a variety of different sources is reported. Examples of wear particles from gas turbine engines, bearing tests, friction and wear tests, hydraulic systems, and human joints are illustrated. In addition, the separation of bacteria and human cells is described.

INTRODUCTION

Spectrometric analysis (ref. 1) has been used for many years to monitor the wear metal content of used lubricants. Other techniques include particle counters, vibration monitors and magnetic chip detectors. These techniques all suffer from the disadvantage of not being able to determine which wear mode is producing the wear debris.

In 1972, Seifert and Westcott (ref. 2) introduced a technique capable of elucidating the wear modes occuring in a wearing system. This is accomplished by precipitating the wear particles from a used lubricant onto a glass slide (Analytical Ferrograph) or inside a glass tube (Direct Reading Ferrograph). The precipitation is accomplished by passing the used lubricant through the tube or over the slide in the presence of a high gradient magnetic field.

Ferrography has been used for the condition monitoring of gas turbine engines (refs. 3 and 4), earth-moving equipment (ref. 5), diesel engines (refs. 6 and 7) and hydraulic systems (refs. 8 and 9). This technique has also been used in a variety of fundamental wear mechanism studies (refs. 10 to 14) and in certain medical applications (refs. 15 to 18).

The objective of this paper is to review the occurrence of various types of wear particles and lubricant contaminants and to discuss the processes responsible for their generation.

APPARATUS

Ferroscope

The Ferroscope used in this study is a Richert Zetopan large research microscope equipped with a bichromatic illumination system, a camera and a photodetector. The system provides for both transmitted green light and reflected red light simultaneously. This high contrast combination makes it possible to distinguish light transmitted through particles from light reflected by the surfaces of the particles. Opaque particles return the reflected light and appear red. Transparent particles reflect little light but pass the transmitted light and appear green. The microscope is also equipped with polarizers which allow examination of particles in reflected

E-1648

polarized light. This yields information concerning the optical activities of the particles. The photodetector is used to measure the amount of particles at various locations on a Ferrogram.

Scanning Electron Microscope (SEM)

The SEM used in this study is an ISI-40/4 having a 60 Å resolution with 10 X to 600 000 X magnification range. In addition, the system is equipped with a PGT SYSTEM III energy dispersive x-ray analyzer for elemental particle analysis.

Analytical Ferrograph

The Analytical Ferrograph is an instrument used to magnetically precipitate wear particles from a used oil onto a specially prepared glass slide. A mixture of 3 ml of used oil and 1 ml of solvent is prepared. This mixture is then slowly pumped over the slide as shown in figure 1. A solvent wash and fixing cycle follows which removes residual oil and permanently attaches the particles to the slide. The resulting slide with its associated particles is called a Ferrogram. A sketch of a Ferrogram slide is illustrated in figure 2.

REGIMES OF LUBRICATION

Stribeck-Hersey Curve

Before discussing the types of wear particles it would be appropriate to point out the various regimes of lubrication. The classical way of depicting some of these regimes is by the well-known Stribeck-Hersey curve (refs. 19 and 20) shown in figure 3. The coefficient of friction is plotted as a function of a dimensionless parameter ZN/P, where Z is viscosity, N is speed and P is the load.

At high values of ZN/P which occur at high speeds, low loads, and at high viscosities, the surfaces are completely separated by a thick (>0.25 μm) ($>10^{-5}$ in.) lubricant film. This is the area of hydrodynamic lubrication where friction is determined by the rheology of the lubricant. For nonconformal concentrated contacts where loads are high enough to cause elastic deformation of the surfaces and pressure-viscosity effects on the lubricant, another fluid film regime, elastohydrodynamic lubrication (EHD), can be identified. In this regime film thicknesses (h) may range from (0.025 to 2.5 μm) (10^{-6} to 10^{-4} in.).

As film thickness becomes progressively thinner, surface interactions start taking place. This regime of increasing friction, in which there is a combination of asperity interactions and fluid film effects, is referred to as the mixed lubrication regime. Finally, at low values of the ZN/P parameter, one enters the realm of boundary lubrication.

Wear vs Load

All of the regimes depicted in the Stribeck-Hersey curve can also be illustrated in an idealized plot of wear versus load (fig. 4). Here, in

addition to hydrodynamic, EHD, mixed and the boundary regime, transitions to severe wear and seizure are illustrated.

WEAR PARTICLES AND SURFACE DAMAGE

Reda, et al. (ref. 21) have reported on the types of wear particles and surface damage that ensues as load is continually increased for a lubricated steel on steel sliding couple (similar to the plot of fig. 4).

Hydrodynamic and EHD Regimes

Since the surfaces are completely separated in these regimes, no wear or surface damage should be evident. This is the case with a featureless surface (fig. 5(a)) with only a few isolated wear particles (fig. 5(b)), probably due to start-up or shut-down.

Mixed and Boundary Lubrication Regimes

These are mild wear regimes where penetration of the boundary film occurs. This produces the surface damage as illustrated in figure 6(a). Wear particles are generated in a thin surface layer that is continuously removed and reformed during the sliding process. In Ferrographic terminology these wear particles are referred to as normal rubbing wear particles. These flake-like particles are released into the lubricant by an exfoliation or fatigue-like process. The rate of removal of this surface layer is less than its rate of formation. Wear occurs continuously, but at a low rate.

These wear particles are arranged in strings by the magnetic field of the Ferrograph (fig. 6(b)). A scanning electron micrograph (fig. 7) (ref. 11) at a higher magnification illustrates their flake-like nature. Typically, for steel surfaces, these particles are 0.75 to 1.0 μm in thickness with a major dimension of less than 15 μm.

The transition from the EHD regime into the mixed and boundary regimes is dramatically illustrated by Ferrographic analysis (fig. 8) (ref. 11). In this figure, the Ferrogram density is plotted as a function of λ which is the ratio of the film thickness to the composite surface roughness. This data was generated by sliding steel balls of three different roughnesses against a sapphire plate. As can be seen, the amount of wear debris increases sharply at λ values of one and below where surface interactions begin taking place.

Transition to Severe Wear

As load is increased, there is some point (Y) (fig. 4) where the rate of removal of the surface layer starts to exceed its rate of formation. A transition from mild to severe wear occurs. Surface damage becomes more extensive (fig. 9(a)). As the surface film starts to fail, much larger metallic wear particles (up to 150 μm in major dimension) are formed (fig. 9(b)).

Failure

Finally, at very high loads, complete breakdown of the protective surface occurs. Considerable smearing and tearing of the surface is evident with grooving to 200 μm (fig. 10(a)). Free metallic particles having dimensions up to 1 mm are generated (fig. 10(b)).

OTHER TYPES OF WEAR PARTICLES

So far only normal rubbing wear and some severe wear particles have been described. There are a number of other distinct types.

Abrasive Wear

Abrasive or cutting wear occurs when a hard surface or a hard particle abrades a softer surface. The particles formed are very similar to those produced by a lathe, only on a microscale. Typically, these particles are 2–5 μm wide and 25–100 μm long. Examples of this wear particle type are illustrated in figure 11.

The presence of abrasive contaminants or abrasive wear debris in a lubrication system may cause the generation of much finer (thicknesses to 0.25 μm) wire-like debris (ref. 22). In any case, the occurrence of abrasive wear debris indicates an abnormal wear mode.

Rolling Element Fatigue

Rolling element bearings generate three particle types related to fatigue. First, fatigue spall fragments are observed. This is the material released when a spall opens up. Typically, these particles are flat, irregularly shaped, platelets initially up to 100 μm in size. They have a major dimension to thickness ratio of about 10 to 1. These particles are similar in morphology to normal rubbing wear particles, only larger. Examples of this type particle appear in figure 12.

Particles thought to be related to rolling element fatigue are metallic microspheres. They resemble miniature ball bearings and are of the order of 1 to 5 μm in diameter. Presumably, they are generated in propagating fatigue cracks. When these cracks reach the surface, spheres are released into the oil. Our work (fig. 13) has shown an increase in sphere count just prior to failure as detected by accelerometers (ref. 12). Earlier work (ref. 13) involving accelerated rolling element fatigue tests yielded mixed results. Some tests yielded increases in sphere counts while in others few spheres were detected. An example of a sphere from a rolling element fatigue test appears in figure 14.

A third particle type is sometimes observed during rolling element fatigue. These are large (20–50 μm in major dimension) laminar particles having a thickness ratio of about 30 to 1. They are probably formed by the passage of a wear particle through a rolling contact.

Iron Oxide Particles

Occasionally, because of water contamination or other reasons, a spectrometer oil analysis (SOAP) will indicate large quantities of iron in a

lubricant. However, after precipitation by the Ferrograph, it is evident that most of the iron is in the form of oxides or rust (fig. 15). This condition, which should be rectified, is not nearly as serious as one in which all of the iron would be in the form of wear debris.

However, under certain conditions a mild form of oxidative wear can occur. Here, the majority of particles are iron oxide of the α-Fe_2O_3 type. Under more severe conditions, black oxide particles consisting of γ-Fe_2O_3, Fe_3O_4 and FeO predominate.

Both of these oxidative wear regimes are most commonly observed during unlubricated conditions. However, both regimes have been observed during lubricated sliding which is indicative of very poor, perhaps starved, lubrication.

Nonferrous Particles

Nonferrous particles often appear in oil samples. They are the result of wear processes taking place in pumps, hydraulic system components, bearings or other parts containing nonferrous materials in sliding contact. An example of a bronze wear particle is illustrated in figure 16. It was the result of high cage wear in a ball bearing during a fatigue test (ref. 12).

Grinding Particles

Spherical particles may also be produced by grinding operations (ref. 14). In the optical microscope these spheres appear quite similar to spheres related to rolling element fatigue. However, they are usually larger in diameter (>10 μm). SEM examination (fig. 17) reveals that many are hollow and their surface features, both internal and external, indicate that a melting and resolidification process occurred.

Similar spherical particles may be formed as a result of catastrophic failure. Figure 18 reveals a number of spheres produced when a gas turbine engine caught fire and exploded (ref. 3).

Lubricant Breakdown Particles

Some lubricants under sliding contact conditions produce large quantities of an insoluble sludge. This material, which is often referred to as friction polymer, can clog filters, reduce clearances, and reduce the life of the lubricant. An example of this type of debris is shown in figure 19. These particles were generated by a polyphenyl ether during boundary lubrication experiments (ref. 10). These particles are precipitated by the Ferrograph because they do contain some iron from the steel surface. Breakdown products that do not contain iron will not normally appear on a Ferrogram. However, these nonmagnetic particles can be precipitated by using magnetic ion solutions. Their use is described in the next section.

Hydraulic Fluid Analysis

The types of wear particles described thus far are mainly associated with lubrication systems. However, these particles may also be produced in hydraulic systems. Many failures in industrial hydraulic systems are not

predictable by wear particle monitoring alone. Organic debris in the hydraulic fluid may be indicative of seal or gasket failure.

Normally, this nonmagnetic debris will not be precipitated by the Ferrograph. However, the use of magnetizing solutions (ref. 9) which contain rare earth salts can effect precipitation. An example of the use of these solutions is shown in figure 20. In figure 20(a), the percent area covered by debris at various Ferrogram positions for the standard system and the magnetizing system is shown for an initial hydraulic fluid sample. A little more debris is precipitated with the normal solution. However, data for a sample taken later from the same hydraulic system appears in figure 20(b). Now a large amount of additional debris appears with the magnetizing solution indicative of large amounts of organic debris in the sample. Subsequently, a hydraulic system failure occurred which was attributed to the failure of a fluoroelastomer seal.

BIOLOGICAL APPLICATIONS

The same type of magnetizing agent erbium chloride ($ErCl_3$) can be used to precipitate biological debris (refs. 15 and 16). Here, of course, the solutions are designed for aqueous samples. An example of a biological application of these solutions is shown in figure 21. The separation of a micro-organism (Escherichia coli) common to the human intestinal tract from lymphocytes is illustrated. The lymphocytes have varying sizes, but are still completely precipitated by the 30 mm Ferrogram position. In contrast, the E. coli are about uniformly distributed along the entire length of the Ferrogram. Therefore, complete separation has been effected from the 0 to 30 mm position. This is a much better separation than could be obtained by either filtration or centrifugation.

Another example of the differential bonding of the erbium chloride magnetizing solution is shown in figure 22. Here, a solution of human blood cells have been passed over the Ferrogram. Figure represents a cross section of this Ferrogram at the 40 mm position. The magnetizing solution is preferentially absorbed by the white blood cells (WBC). In contrast, the red blood cells (RBC) absorb little or none of the solution. In fact, the RBC have a magnetic susceptibility less than the solution and are repelled by the magnet. Most of the RBC simply run off the Ferrogram to waste, although a few are pushed to the outside of the Ferrogram track.

Finally, magnetizing solutions have been used to precipitate wear particles and other debris from both natural and artificial human joints (ref. 15). One example is shown in figure 23. Here, a sample of aspirated synovial fluid from an arthroplastic joint was Ferrographically analyzed. This group of particles, photographed with polarized light, was identified as poly (methylmethacrylate). This is the material used to cement prosthetic components into bone. Its presence in the synovial fluid is certainly deleterious to the artificial joint. This rather hard material will abrade both the metal and plastic joint components.

An example of metallic debris isolated from synovial fluid from a total hip replacement appears in figure 24. The metal particle is embedded in a piece of synovial tissue. Analysis of the metal particle indicated that its probable source was from a hemostat during surgery. Apparently hemostats shed such particles due to repeated sterilizations.

Other particles have been isolated from normal human joints including bone, cartilage, and mineral deposits (refs. 17 and 18). The use of Ferrography in diagnosing arthritic diseases and determining the wear patterns in normal and artifical joints is now in its infancy.

CONCLUDING REMARKS

It has been shown that the Ferrograph can effectively isolate wear particles and contaminants from a variety of different types of operating equipment. In addition, its efficiency in separating biological components has been demonstrated. The relationship of these particles to the various wear mechanisms was also discussed. A detailed compilation of most of the types of wear particles described in this paper appears in the Wear Particle Atlas (ref. 22).

REFERENCES

1. Beerbower, A.: Spectrometry and Other Analysis Tools for Failure Prognosis. Lubr. Eng., vol. 32, no. 6, June 1976, pp. 285-293.
2. Seifert, W. W.; and Westcott, V. C.: A Method for the Study of Wear Particles in Lubricating Oil. Wear, vol. 21, 1972, pp. 27-42.
3. Jones, W. R., Jr.: Ferrographic and Spectrometer Oil Analysis From a Failed Gas Turbine Engine, NASA TM-82956, 1982.
4. Scott, D.; McCullagh, P. G.; and Mills, G. H.: Condition Monitoring of Gas Turbine by Ferrographic Trend Analysis. Fundamentals of Tribology, eds. N. P. Suh and N. Saka. MIT. Press, 1980, pp. 869-876.
5. Westcott, V. C.: Ferrography Oil and Grease Analysis as Applied to Earth Moving Machinery. SAE Preprint 7050555, 1978.
6. Jones, M. H.: Ferrography Applied to Diesel Engine Oil Analysis. Wear, vol. 56, 1979, pp. 93-104.
7. Hofman M. V.; and Johnson, J. H.: The Development of Ferrography as a Laboratory Wear Measurement Method for the Study of Engine Operating Conditions on Diesel Engine Wear. Wear, vol. 44, 1977, pp. 183-199.
8. Wear in Fluid Power Systems. Fluid Power Research Center, Okla State Univ. Report No. ONR CR 169-004-2.
9. Bowen, E. R.; and Anderson, D.P.: Ferrographic Analysis of Aqueous/ Glycol Type Lubricants and Hydraulic Fluids, presented at the 36th National Conference on Fluid Power, Oct. 28-30, 1980, Cleveland, Ohio, pp. 199-204. (Illinois Institute of Technology is publisher.)
10. Jones, William R., Jr.: Ferrographic Analysis of Wear Debris from Boundary Lubrication Experiments with a Five Ring Polyphenyl Ether. ASLE Trans., vol. 18, no. 3, 1975, pp. 153-162.
11. Jones, William R., Jr.: Nagaraj, H. S.; and Winer, Ward O.: Ferrographic Analysis of Wear Debris Generated in a Sliding Elastohydrodynamic Contact. ASLE Trans., vol. 21, no. 3, 1978, pp. 181-190.
12. Jones, William R., Jr.; and Loewenthal, Stuart H.: Analysis of Wear Debris from Full-Scale Bearing Fatigue Tests Using the Ferrograph. ASLE Trans., vol. 24, no. 3, 1981, pp. 323-330.
13. Jones, William R., Jr.; and Parker, Richard J.: Ferrographic Analysis of Wear Debris Generated in Accelerated Rolling Element Fatigue Tests. ASLE Trans., vol. 22, no. 1, 1977, pp. 37-45.

14. Jones, W. R., Jr.: Spherical Artifacts on Ferrograms. Wear, vol. 37, 1976, pp. 193-195.
15. Mears, D. C.; Handley, E. N., Jr.; Rutkowski, R.; and Westcott, V. C.: Ferrographic Analysis of Wear Particles in Arthroplastic Joints. J. Biomed. Matl. Res., vol. 12, 1978, pp. 867-875.
16. Russell, A. P.; Demaria, A.; Johns, M.; and Westcott, V. C.: The Concentration and Separation of Bacteria and Cells by Ferrography. International Conference - Advances in Ferrography, D. Scott, ed. University College, Swansea, UK, 1982, pp. 562-574.
17. Evans, C. H.: Application of Ferrography to the Study of Wear and Arthritis in Human Joints. International Conference - Advances in Ferrography, D. Scott, ed. University College, Swansea, UK, 1982, pp. 575-604.
18. Mills, G. H.; and Hunter, J. A.: A Preliminary Use of Ferrography in the Study of Arthritic Diseases. International Conference - Advances in Ferrography, D. Scott, ed. University College, Swansea, UK, 1982, pp. 605-614.
19. Stribeck, R.: Characteristics of Plain and Roller Bearings. Ziet. V.D.I., vol. 46, 1902.
20. Hersey, M. D.: The Laws of Lubrication of Horizontal Journal Bearings. J. Wash. Acad. Sci., vol. 4, 1914, pp. 542-552.
21. Reda, A. A.; Bowen, R.; and Westcott, V. C.: Characteristics of Particles Generated at the Interface Between Sliding Steel Surfaces. Wear, vol. 34, 1975, pp. 261-273.
22. Bowen, E. R.; and Westcott, V. C.: Wear Particle Atlas. Final Report Contract N00156-74-C1682, Naval Air Engineering Center, July 1976.

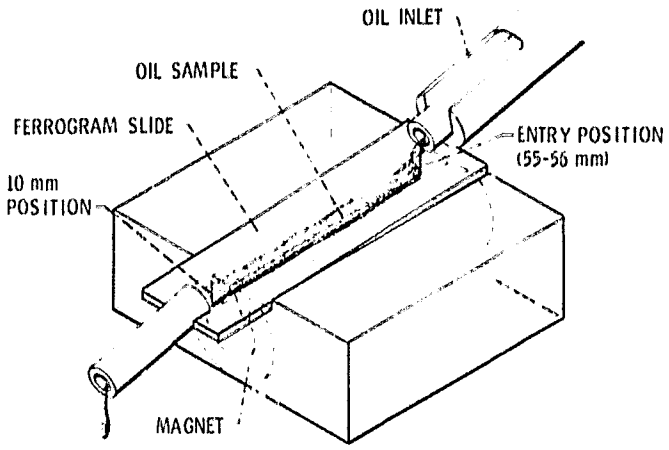

Figure 1. - Analytical ferrograph.

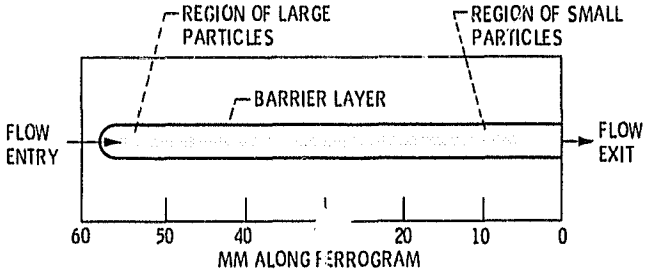

Figure 2. - Ferrogram slide.

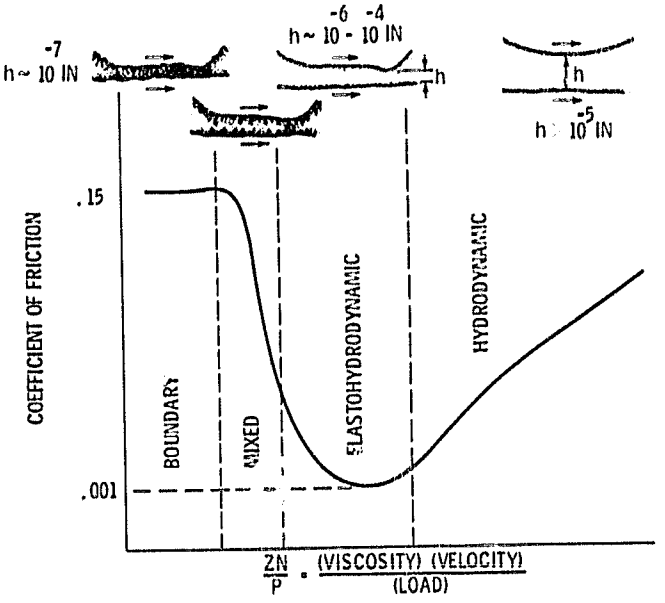

Figure 3. - Coefficient of friction as a function of speed-velocity-load parameter (Stribeck-Hersey curve) (ref. 1).

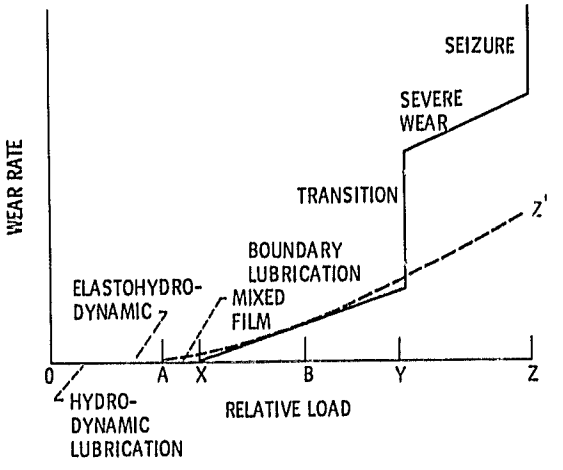

Figure 4. - Wear rate as a function of relative load depicting the various regimes of lubrication (ref. 8).

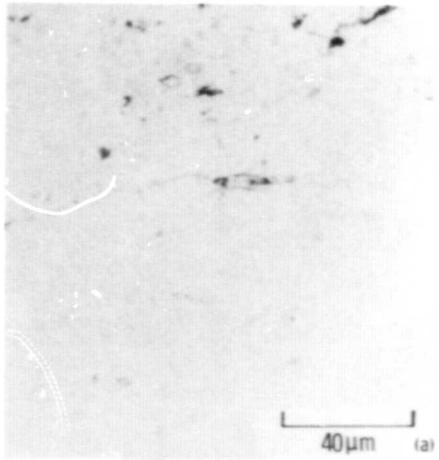

(a) Wear surface.

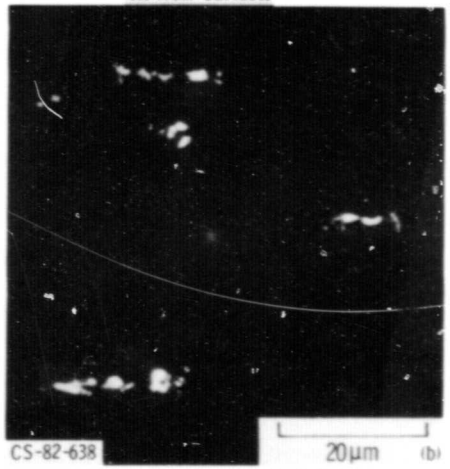

(b) Wear particles (ref. 21).

Figure 5. - Hydrodynamic or elastohydrodynamic lubrication regime.

(a) Wear surface.

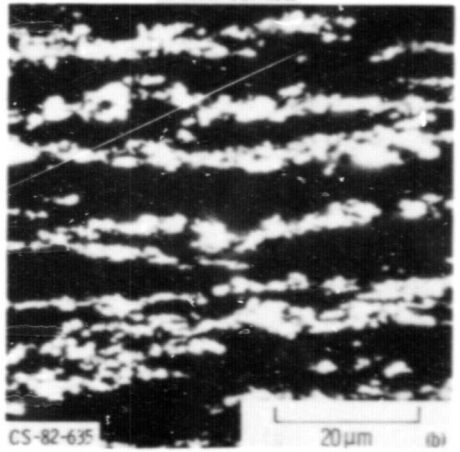

(b) Wear particles (ref. 21).

Figure 6. - Boundary lubrication regime.

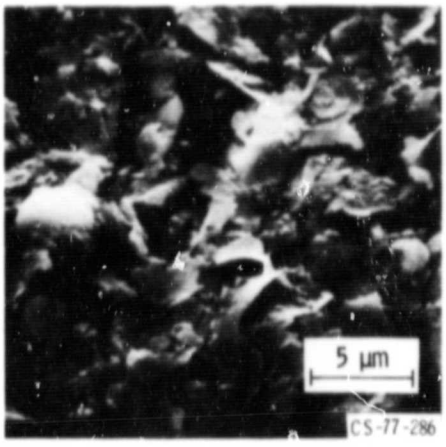

Figure 7. - Normal rubbing wear particles.

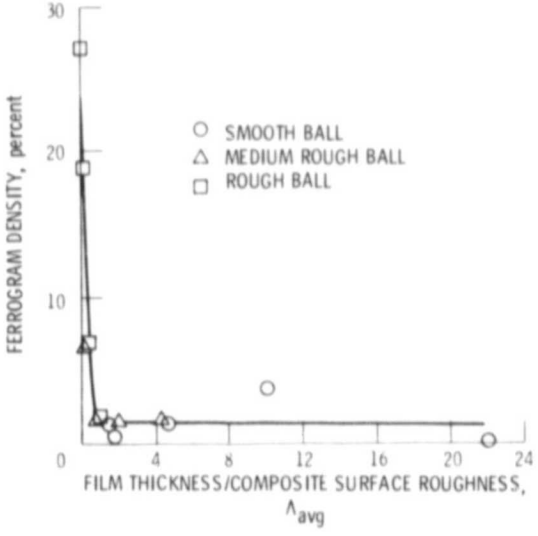

Figure 8. - Ferrogram density versus average Λ ratio (ref. 11).

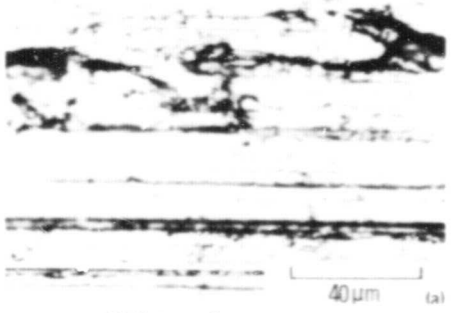

(a) Wear surface.

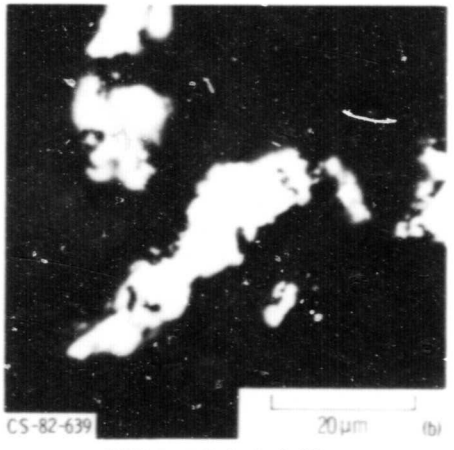

(b) Wear particles (ref. 21).

Figure 9. - Transition to severe wear.

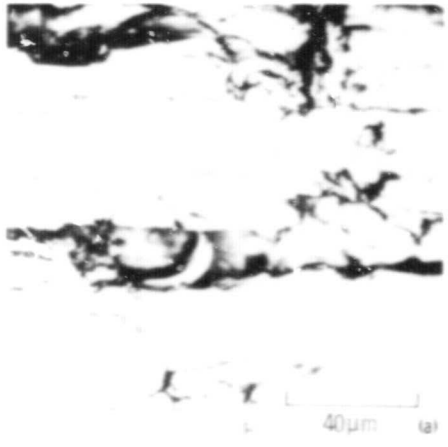

(a) Wear surface.

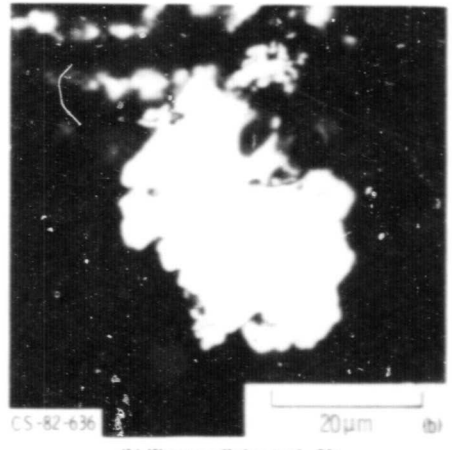

(b) Wear particles (ref. 21).

Figure 10. - Transition to seizure.

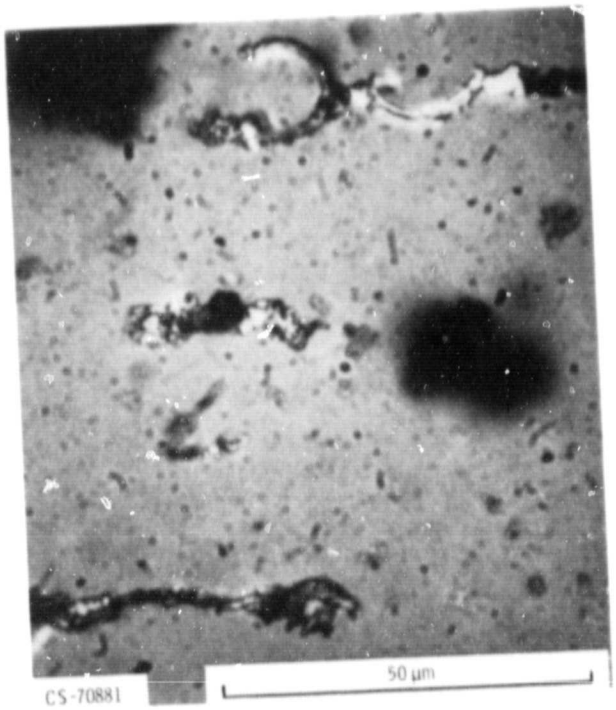

Figure 11. - Abrasive wear debris (from ref. 10).

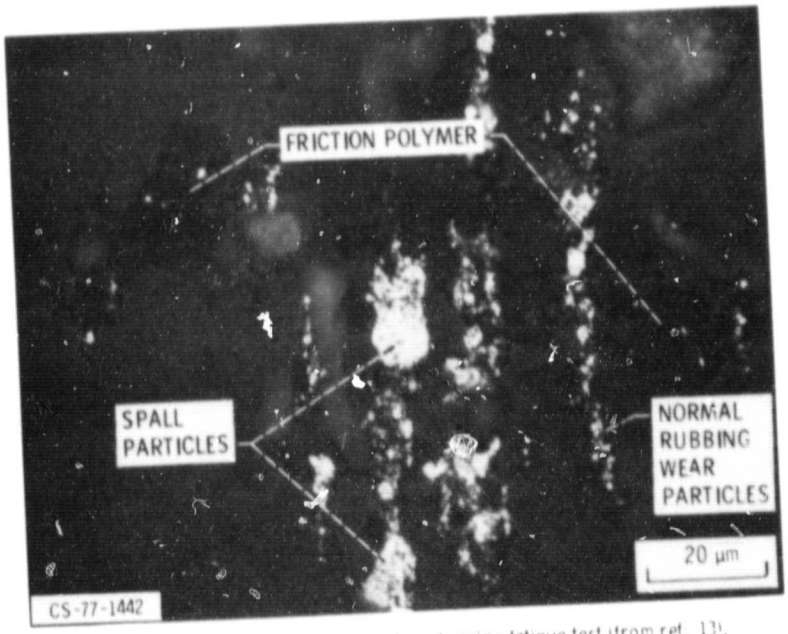

Figure 12. - Ferrogram entry deposit from bearing fatigue test (from ref. 13).

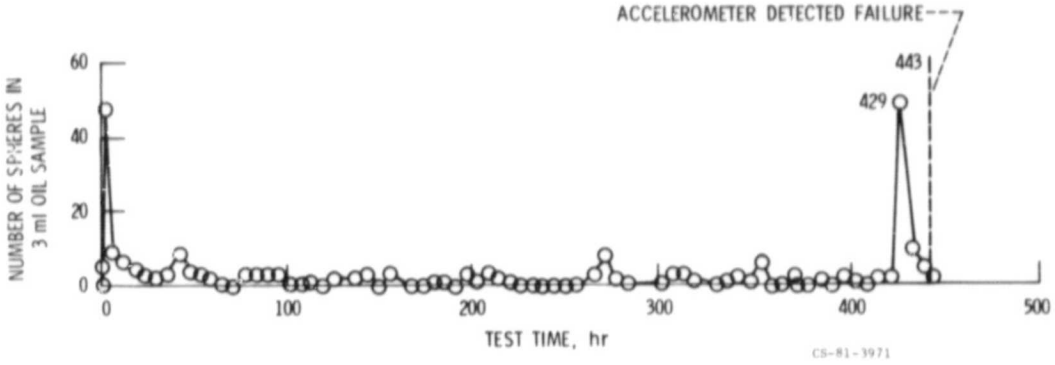

Figure 13 - Number of spheres in 3 ml of oil for full scale bearing fatigue test (from ref. 12).

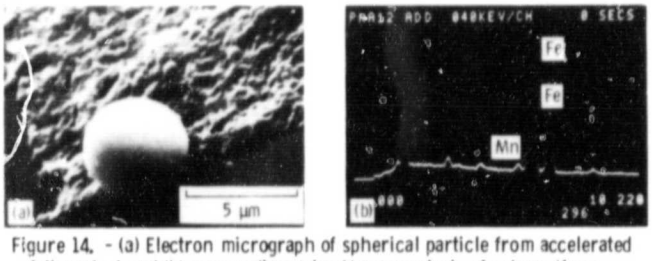

Figure 14. - (a) Electron micrograph of spherical particle from accelerated fatigue test and (b) energy dispersive X-ray analysis of sphere (from ref. 13).

CS-77-1448

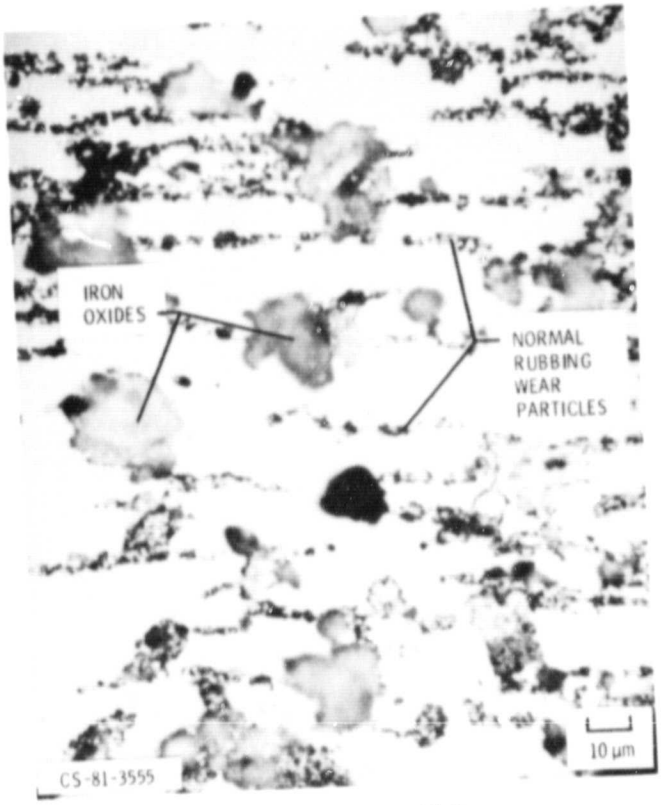

Figure 15. - Iron oxide debris.

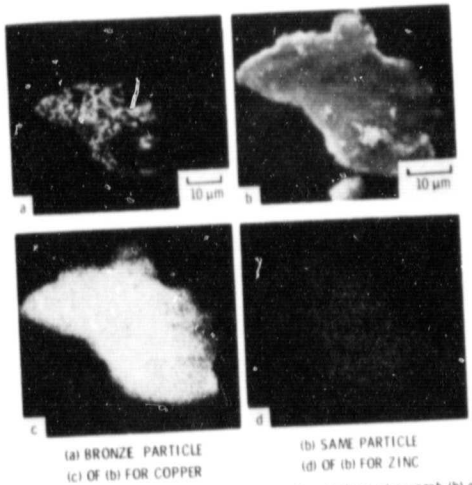

(a) BRONZE PARTICLE
(b) SAME PARTICLE
(c) OF (b) FOR COPPER
(d) OF (b) FOR ZINC

Figure 16. - Optical micrograph (a) and scanning electron micrograph (b) of same particle and their corresponding X-ray energy maps (c) and (d) (Ref. 12).

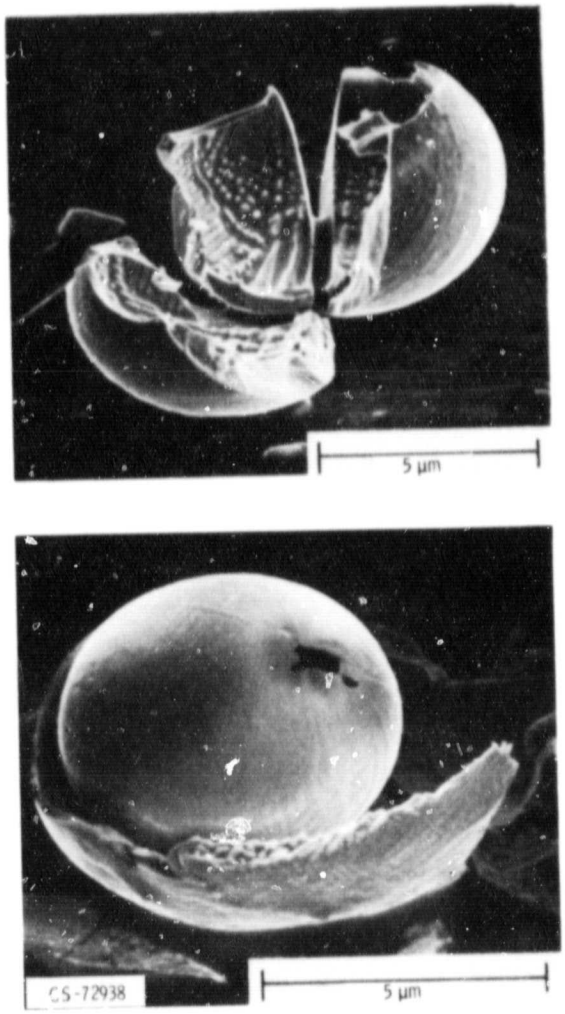

Figure 17. - Scanning electron micrographs of spherical grinding debris (from ref. 14).

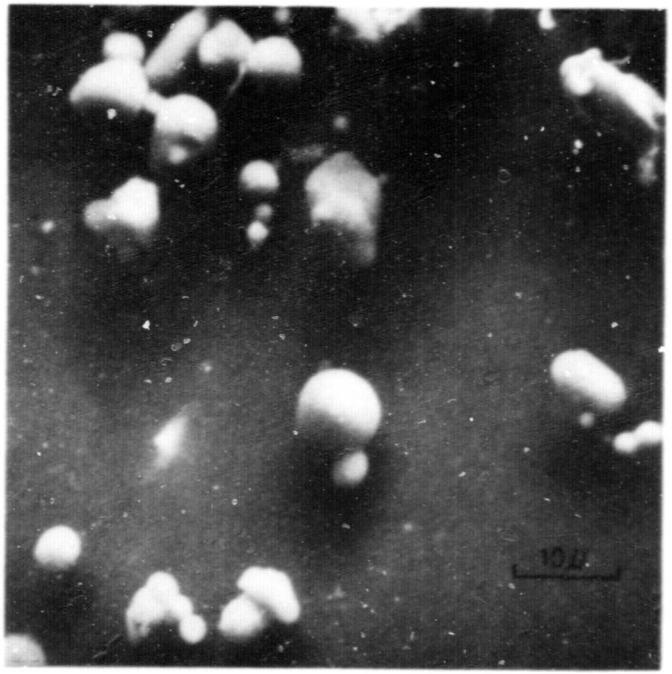

(a) Electron micrograph of debris.

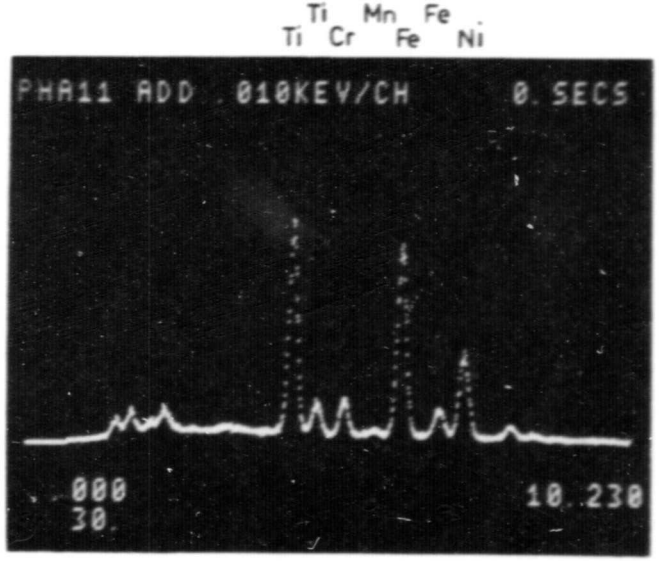

(b) Typical EDX analysis of particle.

Figure 18. - Debris from failed gas turbine engine (ref. 3).

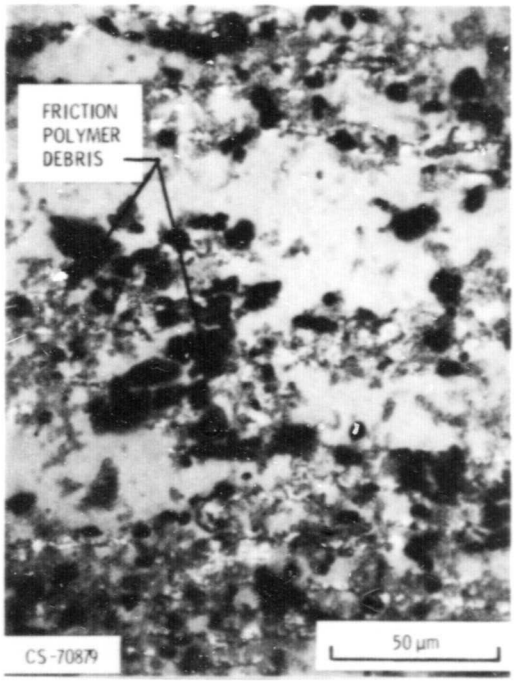

Figure 19. - Friction polymer wear debris (from ref. 10).

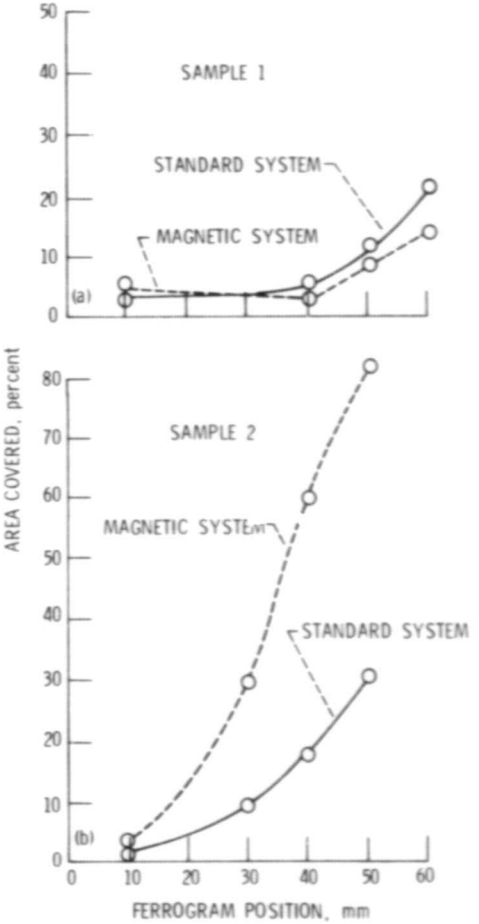

(a) Initial hydraulic fluid sample.

(b) Subsequent hydraulic fluid sample (from ref. 9).

Figure 20. - Percent area covered at various ferrogram positions.

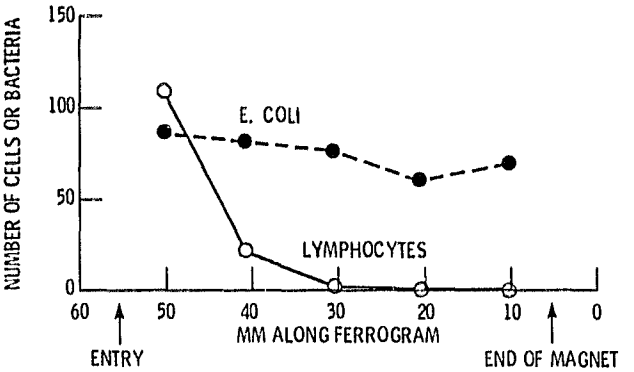

Figure 21 - Ferrographic separation of Escherichia COLI from lymphocytes using erbium chloride magnetizing solution. (Ref 16).

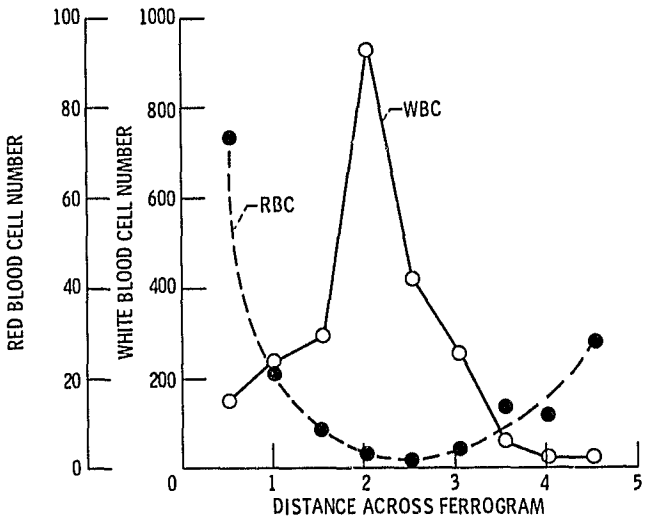

Figure 22 - Concentration of human red and white blood cells across a ferrogram at the 40 mm position (Ref. 16).

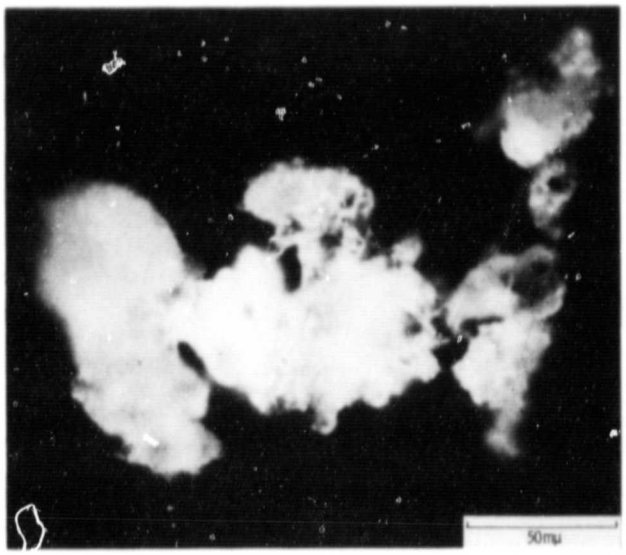

Figure 23. - Poly (Methyl Methacrylate) particles (Bone Cement) precipitated ferrographically from synovial fluid (Ref. 15).

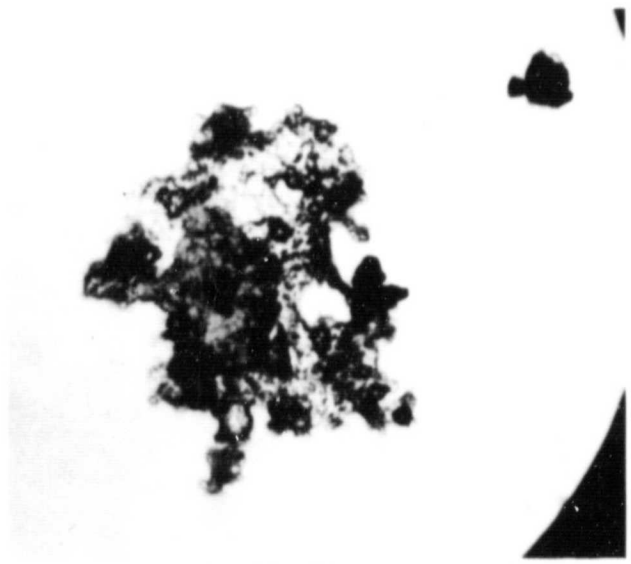

Figure 24. - Ferrogram of a metal particle embedded in synovial tissue from an artificial hip joint.